

Convolutional Neural Network and Adaptive Dictionary Learning for Brain Tumour Cell Detection

N. Poonguzhali, B. Punitha, J. Ashwini Mega, G. Thamizamudhu

Abstract: In this paper, we propose an efficient brain tumor detection method and an automatic segmentation method, which can detect tumor and locate it in the brain MRI images. Automatic and reliable segmentation methods are used in order to manage large spatial and structural variability among brain tumors. Also, some pre-processing steps are used for tumor detection purpose. The automatic segmentation method is based on convolution neural networks. We present an automatic cell detection framework using sparse reconstruction and adaptive dictionary learning. The automatic cell detection results are compared with manually annotated ground truth and other state-of-the-art cell detection algorithms.

Keywords: Cell detection, MRI images.

I. INTRODUCTION

Image processing is processing of images using mathematical operations by using any form of signal processing for which the input is an image, a series of images, or a video, such as a photographer video frame; the output of image processing may be either an image or a set of characteristics or parameters related to the image. Most image-processing techniques involve treating the image as a dimensional signal and applying standard signal-processing techniques to it. Images are also processed as three-dimensional signals where the third-dimension being time or the z-axis. In brain tumor segmentation, we find several methods that explicitly develop a parametric or non-parametric probabilistic model for the underlying data. These models usually include a likelihood function corresponding to the observations and a prior model. Being abnormalities, tumors can be segmented as outliers of normal tissue, subjected to shape and connectivity constraints. Mathematical morphology stresses the role of "shape" in image pre-processing, segmentation and object description. Morphology usually divided into binary mathematical morphology which operates on binary images and gray level images. The two fundamental operations are Dilation and erosion. Dilation expands the object to the closest pixels of the neighborhood.

Revised Version Manuscript Received on April 12, 2017.

Dr. N. Poonguzhali, Assistant Professor, Department of Computer Science and Engineering, Manakula Vinayagar Institute of Technology, Puducherry (Tamil Nadu), India.

B. Punitha, UG student, Department of Computer Science and Engineering, Manakula Vinayagar Institute of Technology, Puducherry (Tamil Nadu), India.

J. Ashwini Mega, UG student, Department of Computer Science and Engineering, Manakula Vinayagar Institute of Technology, Puducherry (Tamil Nadu), India.

G. Thamizamudhu, UG student, Department of Computer Science and Engineering, Manakula Vinayagar Institute of Technology, Puducherry (Tamil Nadu), India.

A. Brain Tumor

A brain tumor or intracranial neoplasm occurs when abnormal cells form within the brain. There are two main types of tumors: malignant or cancerous tumors and benign tumors. Cancerous tumors can be divided into primary tumors that start within the brain, and secondary tumors that have spread from somewhere else, known as brain metastasis tumors.



Fig.1. Brain Tumor

All types of brain tumors may produce symptoms that vary depending on the part of the brain involved. These symptoms may include headaches, seizures, problem with vision, vomiting, and mental changes. The headache is classically worse in the morning and goes away with vomiting. More specific problems may include difficulty in walking, speaking, and with sensation. As the disease progresses unconsciousness may occur.

II. RELATED WORKS

The accurate segmentation of gliomas and its intra-tumoral structures is important not only for treatment planning, but also for follow-up evaluations. However, manual segmentation is time-consuming and subjected to inter- and intra-rater errors difficult to characterize. Thus, physicians usually use rough measures for evaluation [1]. For these reasons, accurate semiautomatic or automatic methods are required [1], [5]. However, it is a challenging task, since the shape, structure, and location of these abnormalities are highly variable. Additionally, the tumor mass effect change the arrangement of the surrounding normal tissues [5]. Also, MRI images may present some problems, such as intensity in homogeneity [6], or different intensity ranges among the same sequences and acquisition scanners [7].

In brain tumor segmentation, we find several methods that explicitly develop a parametric or non-parametric probabilistic model for the underlying data. These models usually include a likelihood function corresponding to the observations and a prior model. Being abnormalities, tumors can be segmented as outliers of normal tissue, subjected to shape and connectivity constrains [8]. Other approaches rely on probabilistic atlases [9]–[11]. In the case of brain tumors, the atlas must be estimated at segmentation time, because of the variable shape and location of the neoplasms [9]–[11]. Tumor growth models can be used as estimates of its mass effect, being useful to improve the atlases [10], [11]. The neighborhood of the voxels provides useful information for achieving smoother segmentations through Markov Random Fields (MRF) [9]. Zhao et al. [5] also used a MRF to segment brain tumors after a first oversegmentation of the image into supervoxels, with a histogram-based estimation of the likelihood function. As observed by Menze et al. [5], generative models generalize well in unseen data, but it may be difficult to explicitly translate prior knowledge into an appropriate probabilistic model.

III. SYSTEM ANALYSIS

A. Existing System

A generative models generalize well in unseen data, but it may be difficult to explicitly translate prior knowledge into an appropriate probabilistic model. Another class of methods learns a distribution directly from the data. Although a training stage can be a disadvantage, these methods can learn brain tumor patterns that do not follow a specific model. This kind of approaches commonly consider voxels as independent and identically distributed, although context information may be introduced through the features. Because of this, some isolated voxels or small clusters may be mistakenly classified with the wrong class, sometimes in physiological and anatomically unlikely locations.

To overcome this problem, some authors include information of the neighborhood by embedding the probabilistic predictions of the classifier into a Conditional Random Field. In summary, we propose a novel CNN-based method for segmentation of brain tumors in MRI images. We start by a pre-processing stage consisting of bias field correction, intensity and patch normalization. After that, during training, the number of training patches is artificially augmented by rotating the training patches, and using samples of HGG to augment the number of rare LGG classes. The CNN is built over convolution layers with small 3×3 kernels to allow deeper architectures.

In designing our method, we address the heterogeneity caused by multi-site multi-scanner acquisitions of MRI images using intensity normalization. We show that this is important in achieving a good segmentation. Brain tumors are highly variable in their spatial localization and structural composition, so we have investigated the use of data augmentation to cope with such variability.

B. Proposed System

Adaptive Dictionary Learning

At training stage, we manually crop many image patches, and each patch contains one cell located in the center. These image patches form an over-complete dictionary, which is

neither robust nor efficient. Considering this factor, we propose to use the k -selection to select a subset of representative patches to build a compact dictionary. In order to further improve the computational efficiency, we only utilize the patches similar to the testing image patches as the dictionary candidates measured by cosine similarity metric.

A cell splitting method based on ellipse fitting using concave points information is reported in [12] to learn a classifier to refine the cell detection results obtained by ellipse fitting. The major challenges in cell detection for the brain tumor data set include shape variation, cell touching or overlapping, and heterogeneous intracellular intensity, and weak cell boundaries. There are three components, including training stage, testing image specific information acquisition, and cell detection using sparse reconstruction with trivial template. In training stage, a set of representative patches are selected from thousands of manually cropped single cell patches. In the testing image specific information acquisition, for a given testing image, a sample patch is cropped and used to find similar patches from the representative patches to form the dictionary. Although the existing methods are able to handle some of these challenges, they fail in simultaneously addressing all of them. Therefore the accurate cell detection in brain tumor histopathological images remains to be a challenging problem

The algorithm consists of the following steps:

- 1) A set of training image patches is collected from images of different brain tumor patients at different ages. k -selection is applied on this dataset to learn a compact cell library.
- 2) Given a testing image, a testing image specific dictionary is generated by searching in the learned library for similar cells. Cosine distance based on local steering kernel features is employed as the similarity measurement.
- 3) The sparse reconstruction using trivial templates is applied to handle touching cells. A probability map is obtained by comparing the sparsely reconstructed image patch to each testing window.
- 4) A weighted mean-shift clustering is used to generate the final cell detection results.

C. System Architecture

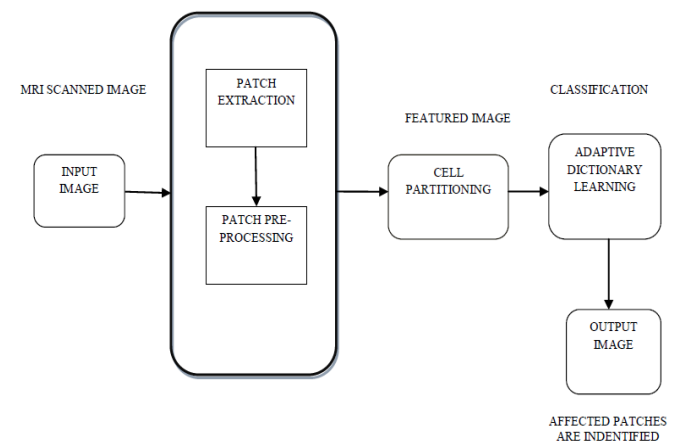


Fig 2. System Architecture

IV. IMPLEMENTATION AND RESULTS

A. GUI Creation

GUI provide point-and-click control of software applications. It integrates the two primary tasks of app building—laying out the visual components and programming app behavior.

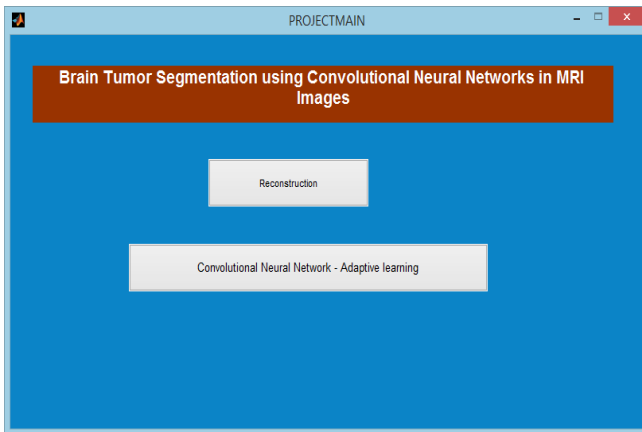


Fig 3. GUI

B. Input Image

The MRI Scanned image is given as input. Functional MRI measures signal changes in the brain that are due to changing neural activity. MRI images may present some problems, such as intensity in homogeneity, or different intensity ranges among the same sequences and acquisition scanners. The shape, structure and location of these abnormalities are highly variable. The mean intensity value and standard deviation across all training patches extracted for each sequence.

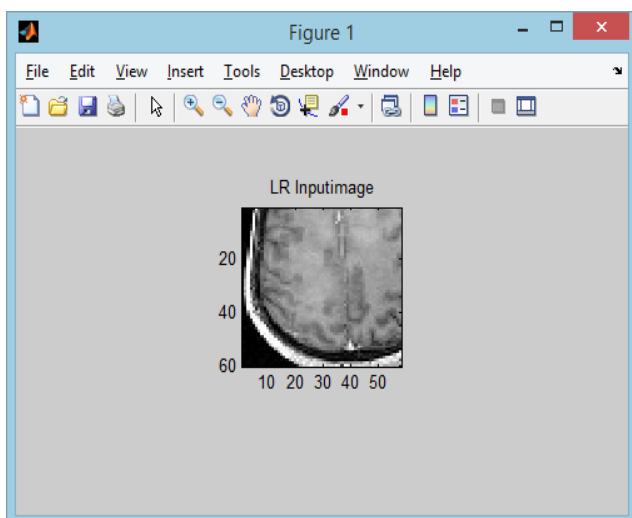


Fig 4. MRI Scanned Image

C. Ground Truth Image

Super resolution offers an effective approach to boost quality and details of low-resolution images to obtain high resolution image. Evaluation result demonstrate the special characteristics of the captured ground truth HR-LR images. The patches with touching/occlusion cells exhibit unexpected appearances in the background such that they are not consistent with the dictionary atoms and thus sparse reconstruction with could result in larger reconstruction errors.

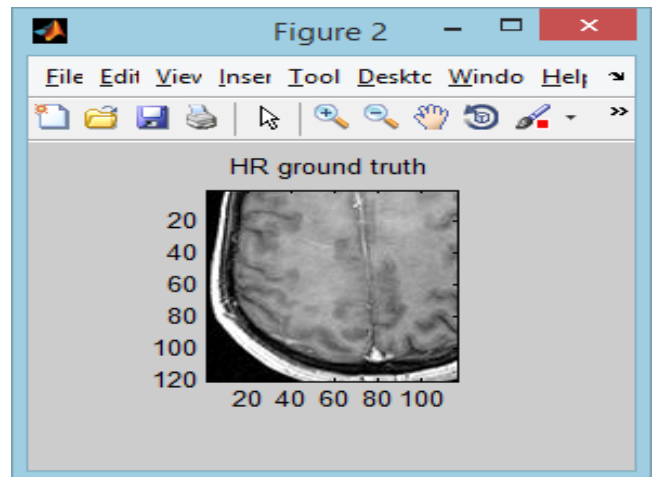


Fig 5. HR Ground Truth

D. Cubic Spline

The spline is constructed of piecewise third-order polynomials which pass through a set of control points. The method involves cluster analysis, that is, grouping the crude data into clusters and seed points are the limits of each cluster. The central for each cluster become nodes through which a natural spline is fitted. B-splines is utilized to infer the object shapes and missing object boundaries. However, the method may not work well on cells with heterogeneous intensity and cluttered background.

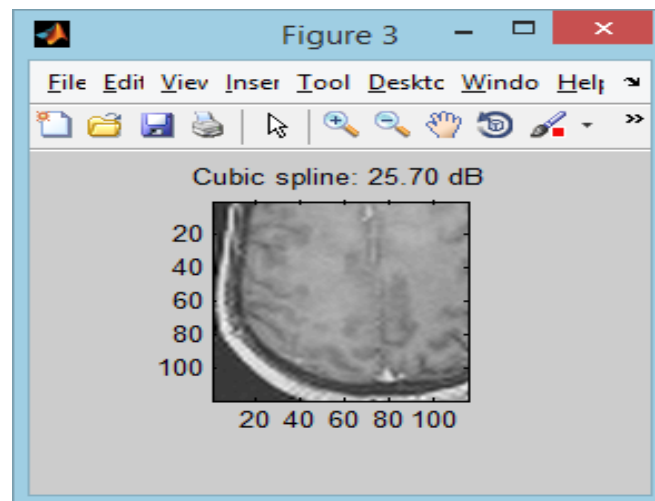


Fig 6. Cubic Spline

E. Sparse Reconstructed Image

The cells with similar appearances approximately lie in the same low dimensional subspace. Each atom corresponds to one training patch with one single non-touching cell at its center, the atoms can sufficiently represent a testing patch with a centered single non-touching cell. The sparse Reconstruction using trivial templates are very similar to the original image. In addition, compared to the original patches it is clear that the clean image not only preserves the original shape of the cell but also removes the touching cells (occlusions). This is due to the contribution of the trivial templates. Using the reconstruction images provides better cell detection results, Because it gives much smaller sparse reconstruction errors even there exist occlusions.

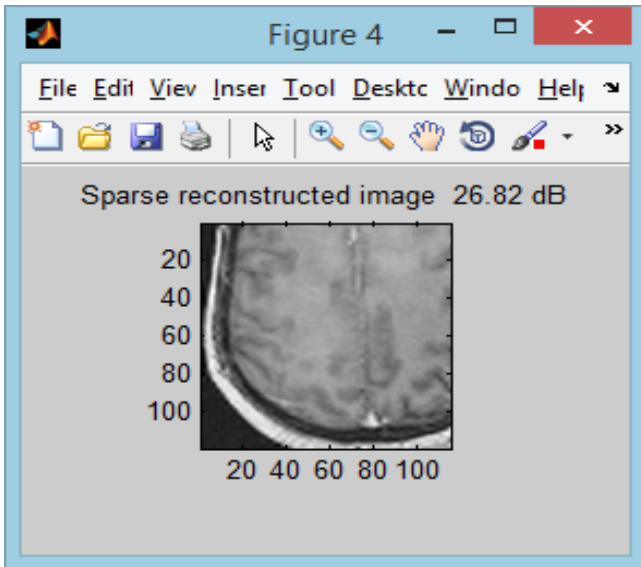


Fig 7. Sparse Reconstructing Image

F. Validation Performance

This structure contains all of the information concerning the training of the network. The error reduces after more epochs of training, but might start to increase on the validation data set as the network starts over-fitting the training data. In the default setup, the training stops after six consecutive increases in validation error, and the best performance is taken from the epoch with the lowest validation error.

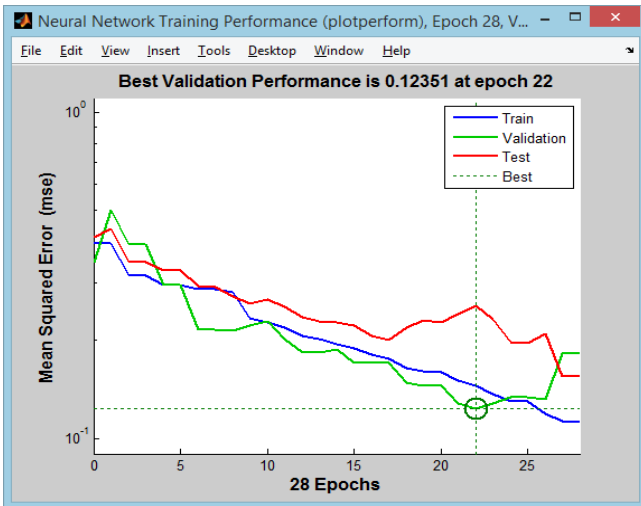


Fig 8. Best Validation Performance

G. Training State

When the network weights and biases are initialized, the network is ready for training. The multilayer feed-forward network can be trained for function approximation (nonlinear regression) or pattern recognition. The process of training a neural network involves tuning the values of the weights and biases of the network to optimize network performance, as defined by the network performance function net. Perform Fcn. There are two different ways in which training can be implemented: incremental mode and batch mode. In incremental mode, the gradient is computed and the weights are updated after each input is applied to the network. In batch mode, all the inputs in the training set are applied to the network before the weights are updated.

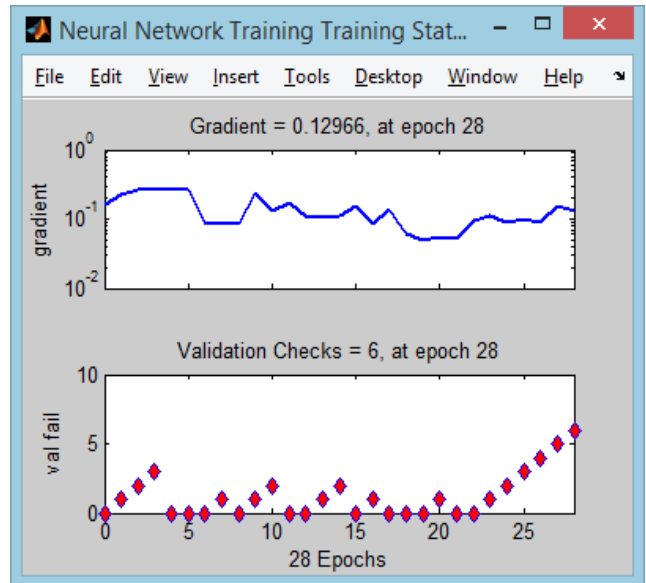


Fig 9. Neural Network Training State

H. Confusion Matrix

On the confusion matrix plot, the rows correspond to the predicted class (Output Class), and the columns show the true class (Target Class). The diagonal cells show for how many (and what percentage) of the examples the trained network correctly estimates the classes of observations. That is, it shows what percentage of the true and predicted classes match. The off diagonal cells show where the classifier has made mistakes. The column on the far right of the plot shows the accuracy for each predicted class, while the row at the bottom of the plot shows the accuracy for each true class. The cell in the bottom right of the plot shows the overall accuracy.

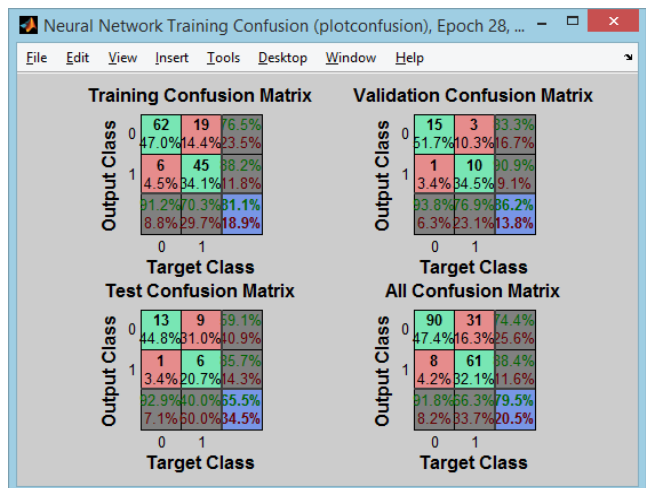


Fig 10. Confusion Matrix

V. CONCLUSION

This paper presents an efficient method of classifying MR brain images into normal, benign and malignant tumor, using an adaptive learning. We propose a novel CNN-based method for segmentation of brain tumors in MRI images. We start by a pre-processing stage consisting of bias field correction, intensity and patch normalization.



The proposed approach gives very promising results in classifying MR images. Most of the existing methods can detect and classify MR brain images only into normal and abnormal. Based on the experimental results, adaptive learning is considered to major advantages over conventional neural networks, due to the fact that adaptive learning learns from the training data instantaneously.

REFERENCES

1. S. Bauer et al., "A survey of mri-based medical image analysis for brain tumor studies," *Physics in medicine and biology*, vol. 58, no. 13, pp. 97–129, 2013.
2. N. Louis et al., "The 2007 who classification of tumours of the central nervous system," *Acta neuropathologica*, vol. 114, no. 2, pp. 97–109, 2007.
3. G. Van Meir et al., "Exciting new advances in neuro-oncology: The avenue to a cure for malignant glioma," *CA: a cancer journal for clinicians*, vol. 60, no. 3, pp. 166–193, 2010.
4. Tabatabai et al., "Molecular diagnostics of gliomas: the clinical perspective," *Acta neuropathologica*, vol. 120, no. 5, pp. 585–592, 2010.
5. Menze et al., "The multimodal brain tumor image segmentation benchmark (brats)," *IEEE Transactions on Medical Imaging*, vol. 34, no. 10, pp. 1993–2024, 2015.
6. N. J. Tustison et al., "N4itk: improved n3 bias correction," *IEEE Transactions on Medical Imaging*, vol. 29, no. 6, pp. 1310–1320, 2010.
7. L. G. Nyul, J. K. Udupa, and X. Zhang, "New variants of a method of mri scale standardization," *IEEE Transactions on Medical Imaging*, vol. 19, no. 2, pp. 143–150, 2000.
8. M. Prastawa et al., "A brain tumor segmentation framework based on outlier detection," *Medical image analysis*, vol. 8, no. 3, pp. 275–283, 2004.
9. H. Menze et al., "A generative model for brain tumor segmentation in multi-modal images," in *Medical Image Computing and Computer-Assisted Intervention–MICCAI 2010*. Springer, 2010, pp. 151–159.
10. Gooya et al., "Glistr: glioma image segmentation and registration," *IEEE Transactions on Medical Imaging*, vol. 31, no. 10, pp. 1941–1954, 2012.
11. Kwon et al., "Combining generative models for multifocal glioma segmentation and registration," in *Medical Image Computing and Computer-Assisted Intervention–MICCAI 2014*. Springer, 2014, pp. 763–770.
12. S. Bauer, L.-P. Nolte, and M. Reyes, "Fully automatic segmentation of brain tumor images using support vector machine classification in combination with hierarchical conditional random field regularization," in *Medical Image Computing and Computer-Assisted Intervention–MICCAI 2011*. Springer, 2011, pp. 354–361.
13. C.-H. Lee et al., "Segmenting brain tumors using pseudo-conditional random fields," in *Medical Image Computing and Computer-Assisted Intervention–MICCAI 2008*. Springer, 2008, pp. 359–366.
14. R. Meier et al., "A hybrid model for multimodal brain tumor segmentation," in *Proceedings of NCI-MICCAI BRATS*, 2013, pp. 31–37.
15. "Appearance-and context-sensitive features for brain tumor segmentation," in *MICCAI Brain Tumor Segmentation Challenge (BraTS)*, 2014, pp. 20–26.
16. Zikic et al., "Decision forests for tissue-specific segmentation of high-grade gliomas in multi-channel mr," in *Medical Image Computing and Computer-Assisted Intervention–MICCAI 2012*. Springer, 2012, pp. 369–376.
17. S. Bauer et al., "Segmentation of brain tumor images based on integrated hierarchical classification and regularization," *Proceedings of MICCAIBRATS*, pp. 10–13, 2012.
18. S. Reza and K. Iftikharuddin, "Multi-fractal texture features for brain tumor and edema segmentation," in *SPIE Medical Imaging*. International Society for Optics and Photonics, 2014, pp. 903 503–903 503.
19. N. Tustison et al., "Optimal symmetric multimodal templates and concatenated random forests for supervised brain tumor segmentation (simplified) with ants," *Neuroinformatics*, vol. 13, no. 2, pp. 209–225, 2015.
20. Geremia, B. H. Menze, and N. Ayache, "Spatially adaptive random forests," in *2013 IEEE 10th International Symposium on Biomedical Imaging (ISBI)*. IEEE, 2013, pp. 1344–1347.
21. Pinto et al., "Brain tumour segmentation based on extremely randomized forest with high-level features," in *Engineering in Medicine and Biology Society (EMBC), 2015 37th Annual International Conference of the IEEE*. IEEE, 2015, pp. 3037–3040.
22. Islam, S. Reza, and K. M. Iftikharuddin, "Multifractal texture estimation for detection and segmentation of brain tumors," *IEEE Transactions on Biomedical Engineering*, vol. 60, no. 11, pp. 3204–3215, 2013.
23. R. Meier et al., "Patient-specific semi-supervised learning for postoperative brain tumor segmentation," in *Medical Image Computing and Computer-Assisted Intervention–MICCAI 2014*. Springer, 2014, pp. 714–721.
24. Y. Bengio, A. Courville, and P. Vincent, "Representation learning: A review and new perspectives," *Pattern Analysis and Machine Intelligence, IEEE Transactions on*, vol. 35, no. 8, pp. 1798–1828, 2013.
25. Y. LeCun, Y. Bengio, and G. Hinton, "Deep learning," *Nature*, vol. 521, no. 7553, pp. 436–444, 2015.
26. Krizhevsky, I. Sutskever, and G. E. Hinton, "Imagenet classification with deep convolution neural networks," in *Advances in neural information processing systems*, 2012, pp. 1097–1105.
27. S. Dieleman, K. W. Willett, and J. Dambre, "Rotation-invariant convolution neural networks for galaxy morphology prediction," *Monthly Notices of the Royal Astronomical Society*, vol. 450, no. 2, pp. 1441–1459, 2015.
28. D. Ciresan et al., "Deep neural networks segment neuronal membranes in electron microscopy images," in *Advances in neural information processing systems*, 2012, pp. 2843–2851.
29. D. Zikic et al., "Segmentation of brain tumor tissues with convolution neural networks," *MICCAI Multimodal Brain Tumor Segmentation Challenge (BraTS)*, pp. 36–39, 2014.
30. Urban et al., "Multi-modal brain tumor segmentation using deep convolution neural networks," *MICCAI Multimodal Brain Tumor Segmentation Challenge (BraTS)*, pp. 1–5, 2014.
31. Davy et al., "Brain tumor segmentation with deep neural networks," *MICCAI Multimodal Brain Tumor Segmentation Challenge (BraTS)*, pp. 31–35, 2014.
32. M. Havaei et al., "Brain tumor segmentation with deep neural networks," arXiv:1505.03540v1, 2015. [Online]. Available: <http://arxiv.org/abs/1505.03540>
33. M. Lyksborg et al., "An ensemble of 2d convolution neural networks for tumor segmentation," in *Image Analysis*. Springer, 2015, pp. 201–211.
34. Rao, M. Sharifi, and A. Jaiswal, "Brain tumor segmentation with deep learning," *MICCAI Multimodal Brain Tumor Segmentation Challenge (BraTS)*, pp. 56–59, 2015.
35. P. Dvořák and B. Menze, "Structured prediction with convolution neural networks for multimodal brain tumor segmentation," *MICCAI Multimodal Brain Tumor Segmentation Challenge (BraTS)*, pp. 13–24, 2015.
36. K. Simonyan and A. Zisserman, "Very deep convolution networks for large-scale image recognition," arXiv preprint arXiv:1409.1556v6, 2014. [Online]. Available: <http://arxiv.org/abs/1409.1556>
37. M. Shah et al., "Evaluating intensity normalization on mris of human brain with multiple sclerosis," *Medical image analysis*, vol. 15, no. 2, pp. 267–282, 2011.
38. L. Nyul and J. Udupa, "On standardizing the mr image intensity scale," *Magnetic Resonance in Medicine*, vol. 42, no. 6, pp. 1072–1081, 1999.
39. Y. LeCun et al., "Backpropagation applied to handwritten zip code recognition," *Neural computation*, vol. 1, no. 4, pp. 541–551, 1989.
40. "Gradient-based learning applied to document recognition," *Proceedings of the IEEE*, vol. 86, no. 11, pp. 2278–2324, 1998.
41. X. Glorot and Y. Bengio, "Understanding the difficulty of training deep feedforward neural networks," in *International conference on artificial intelligence and statistics*, 2010, pp. 249–256.
42. K. Jarrett et al., "What is the best multi-stage architecture for object recognition?" in *Computer Vision, 2009 IEEE 12th International Conference on*. IEEE, 2009, pp. 2146–2153.
43. L. Maas, A. Y. Hannun, and A. Y. Ng, "Rectifier nonlinearities improve neural network acoustic models," in *Proc. ICML*, vol. 30, 2013.
44. N. Srivastava et al., "Dropout: A simple way to prevent neural networks from overfitting," *The Journal of Machine Learning Research*, vol. 15, no. 1, pp. 1929–1958, 2014.
45. E. Hinton et al., "Improving neural networks by preventing co-adaptation of feature detectors," arXiv preprint arXiv:1207.0580v1, 2012.

- [Online]. Available: <http://arxiv.org/abs/1207.0580>
46. M. Kistler et al., "The virtual skeleton database: An open access repository for biomedical research and collaboration," *Journal of Medical Internet Research*, vol. 15, no. 11, Nov 2013.
 47. VirtualSkeleton, BRATS 2013, 2013. [Online]. Available: <https://www.virtualskeleton.ch/BRATS/Start2013> [Accessed: September 30, 2015]
 48. Bastien et al., "Theano: new features and speed improvements," *Deep Learning and Unsupervised Feature Learning NIPS 2012 Workshop*, 2012.
 49. Bergstra et al., "Theano: a CPU and GPU math expression compiler," in *Proceedings of the Python for Scientific Computing Conference (SciPy)*, Jun. 2010.